

Article

Rheological Properties of Cemented Paste Backfill with Alkali-Activated Slag

Yunpeng Kou^{1,2}, Haiqiang Jiang^{2,3,*} , Lei Ren³, Erol Yilmaz^{4,*}  and Yuanhui Li³

¹ School of Civil and Resources Engineering, University of Science and Technology Beijing, Beijing 100083, China; kouyunpeng@sd-gold.com

² Backfill Engineering Laboratory, Shandong Gold Mining Technology Co., Ltd., Laizhou 261441, China

³ Key Laboratory of Ministry of Education on Safe Mining of Deep Metal Mines, Northeastern University, Shenyang 110819, China; leiren1997@126.com (L.R.); liyuanhui@mail.neu.edu.cn (Y.L.)

⁴ Department of Civil Engineering, Geotechnical Division, Recep Tayyip Erdogan University, Fener, Rize TR53100, Turkey

* Correspondence: jianghaiqiang@mail.neu.edu.cn (H.J.); erol.yilmaz@erdogan.edu.tr (E.Y.)

Received: 4 February 2020; Accepted: 20 March 2020; Published: 22 March 2020



Abstract: This study investigates the time-dependent rheological behavior of cemented paste backfill (CPB) that contains alkali-activated slag (AAS) as a binder. Rheological measurements with the controlled shear strain method have been conducted on various AAS-CPB samples with different binder contents, silicate modulus (M_s : $\text{SiO}_2/\text{Na}_2\text{O}$ molar ratio), fineness of slag and curing temperatures. The Bingham model afforded a good fit to all of the CPB mixtures. The results show that AAS-CPB samples with high binder content demonstrate a more rapid rate of gain in yield stress and plastic viscosity. AAS-CPB also shows better rheological behavior than CPB samples made up of ordinary Portland cement (OPC) at identical binder contents. It is found that increasing M_s yields lower yield stress and plastic viscosity and the rate of gain in these parameters. Increases in the fineness of slag has an adverse effect on rheological behavior of AAS-CPB. The rheological behavior of both OPC- and AAS-CPB samples is also strongly enhanced at higher temperatures. AAS-CPB samples are found to be more sensitive to the variation in curing temperatures than OPC-CPB samples with respect to the rate of gain in yield stress and plastic viscosity. As a result, the findings of this study will contribute to well understand the flow and transport features of fresh CPB mixtures under various conditions and their changes with time.

Keywords: mine tailings; cemented paste backfill; alkali-activated slag; rheological properties

1. Introduction

Mine backfill is often an integrated part of underground mining for several reasons as follows: tailings disposal, ground stability and/or a working platform for operators [1]. To increase the strength and durability of the backfill material placed in underground mined-out stopes or openings, binding agents are considered as one of the most important ingredients in the mix [2]. There are three major types of mine backfilling: hydraulic fill, rock fill and cemented paste backfill (CPB). CPB consists usually of an engineered mix of processing tailings with a solid percentage of 70–85%, single or double hydraulic binder (usually varies between 2 and 9 wt.%) for sufficient cohesion to prevent liquefaction and to provide mechanical strengths, and finally mixing water (usually varies between 18 and 23 cm) for the desired slump [3–7]. Each component of the produced CPB mixes plays a substantial role during its transportation, placement, curing, and strength acquisition [8,9].

The most used binder within the backfill industry is ordinary Portland cement (OPC) due to its availability and versatility [10]. However, OPC is prone to acid and sulphate attacks as a result

of the relatively high percentages of calcium oxide (CaO) [11]. In addition to this fact, binder costs can comprise up to 75% of the operating costs when OPC is used as a sole binder [12]. To reduce the binder-induced costs, to increase the backfill strength/stability performance, and to develop the resistance to acid and sulphate attacks, numerous efforts in utilizing pozzolanic materials such as pulverized fly ash, silica fume and ground granulated blast furnace slag (slag) for the partial replacement of OPC have been made by researchers [13–16]. However, these studies have indicated that the use of natural and artificial pozzolans as a partial replacement of OPC yields lower early mechanical strength and lower rate of gain in the early mechanical strength [17,18].

In recent years, alkali-activated binders (geopolymers) have gained a good reputation as alternative or supplementary binders to cement because it is more effective than OPC in the reduction of greenhouse emissions [19]. They mainly originate from a chemical reaction between solid aluminosilicate powders (e.g., slag, fly ash, metakaolin, and alkali solution of alkali hydroxide, silicate, or sulphate) and alkaline activators (e.g., a blend of sodium hydroxide SH and sodium silicate SS, generally agreed to be the most effective alkali activator) [20,21]. Alkali-activated binders could be designed to have superior properties compared to cement, namely the development of earlier and higher mechanical strengths [22], better resistance to acids and sulphates [23], and lower heat of cement hydration [24]. Numerous studies [17,18,25–27] have been recently shown to better assess the mechanical, workability and microstructural properties of CPB materials by using alkali-activated slag (AAS) as a binder. These studies have shown that, compared to those made up of OPC, CPB samples containing AAS as binder were found to produce remarkably higher early-age strength and stability.

The rheological properties of CPB mass is greatly affected by several parameters including particle size distribution, chemical composition, liquor and solids density, pH, temperature, admixture, mineralogy, mixing regime, and solids concentration [28–30]. There is an internal friction caused by the interaction of water and solids, which may affect the flow rate of CPB material. At high solid concentrations, the internal friction is great enough to prevent CPB material from flowing unless a minimum pressure is applied [31]. This minimum pressure is called the yield stress. The yield stress changes with a change in solid concentration. As solid concentration increases, the yield stress increases and more particles become non-settling [32]. In general, CPB has a high solid concentration, is extremely viscous, and characterized by an increase in viscosity with shear rate. As the solid concentration increases, the viscosity (defined as a measure of the internal friction of a fluid) of CPB increases evenly [33]. The pumpability of fresh CPB also depends on its rheological properties [34]. Pipeline failures such as blockages and ruptures can happen during pumping of CPB materials having high solid concentration, thereby causing production delays [35]. In fact, blockages and ruptures in the pipeline can be reduced and/or eliminated by adding some chemical admixtures to CPB materials. Admixtures choice is a process of understanding interactions between CPB properties and costs in terms of requirements and safety [36]. CPB's rheological behavior can be also improved by increased flow ability of CPB (the plasticizing effect), water reduction and cement optimization, reduced pumping pressure, diminution of pipe blockage risk, and improved safety, providing 'stop and go' without risk of any blockage in pipeline [30,31,35].

Despite the significant progress made by earlier scientific investigations in understanding the mechanical, rheological and microstructural properties of fresh CPB samples made up of AAS, technical data on time-dependent rheological characteristics of AAS-CPB is quite limited. Therefore, there is an urgent need to substantially increase our knowledge about rheological properties of fresh AAS-CPB samples, since the determination of the pipeline transportation system design as well as manufacturing, operating and placement conditions of CPB materials require a thorough understanding of the rheological behavior of CPB mixtures. In the light of this, this study reported herein aims to assess the effect of the curing temperature, the fineness of slag, silicate modulus (M_s : $\text{SiO}_2/\text{Na}_2\text{O}$ molar ratio: [37,38]), and binder content on rheological properties of AAS-CPB.

2. Experimental Program

2.1. Materials

The materials used in this study include tailings, hydraulic binders, alkaline activators (e.g., SH and SS) and distilled water.

2.1.1. Tailings

In this study, a tailings sample produced from an operational gold mine was used to prepare CPB samples. Particle size distribution of the tailings sample was determined using a Malvern laser Mastersizer 2000 (Malvern Panalytical Ltd, Malvern, UK), as shown in Figure 1. The tailings material has a fines content of 25.6%, which can be classified as a coarse size tailings material. The coefficient of uniformity (C_u) and the coefficient of curvature (C_c) were determined to be 24.3 and 0.81, suggesting that the tailings material was poorly graded.

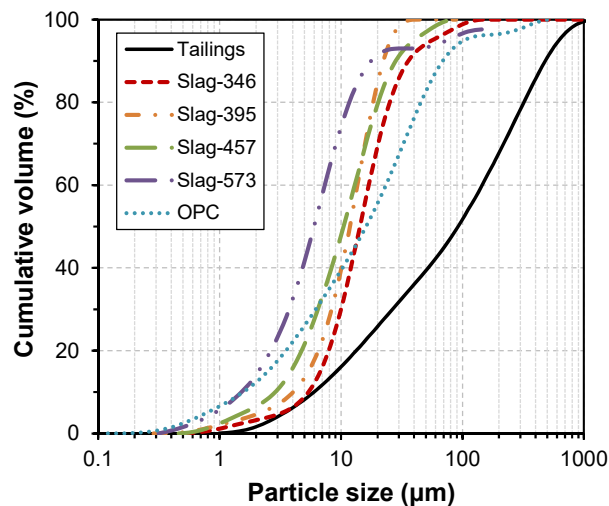


Figure 1. Grain-size distribution curves of tailings and binders.

The mineralogy of tailings was determined by X-ray diffraction (XRD) (Miniflex II, Rigaku Corp., Tokyo, Japan) analysis. The main mineral phase was identified to be quartz, albite and mica. X-ray fluorescence (XRF) analysis indicated that the major chemical composition is SiO_2 (62.5%), Al_2O_3 (16.2%), K_2O (8.11%), Na_2O (3.07%) and CaO (2.98%), along with other trace components (see Figure 2).

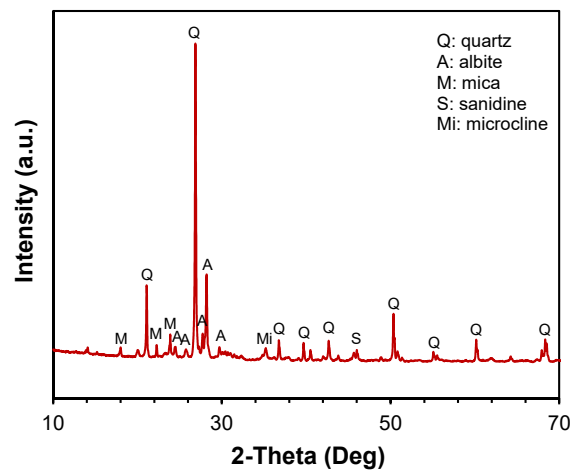


Figure 2. XRD pattern of tailings (from [27]).

2.1.2. Binders and Water

A commercial ordinary Portland cement (OPC) type P·O 52.5R with a Blaine fineness of 415 m²/kg and a specific gravity of 2650 kg/m³ was used as a reference binder. The starting material used to produce the AAS binder is a ground granulated blast furnace slag (slag) from Wuhan iron and steel plant in China. Its Blaine fineness and specific gravity are 346 m²/kg and 2980 kg/m³, respectively. The slag was also ground in a laboratory ball mill until it reached the desired Blaine fineness levels, namely 395, 457 and 573 m²/kg. The chemical composition of slag and cement are given in Table 1. The basicity coefficient ($K_b = (\text{CaO} + \text{MgO})/(\text{SiO}_2 + \text{Al}_2\text{O}_3)$) and the hydration modulus (HM: $\text{CaO} + \text{MgO} + \text{Al}_2\text{O}_3/\text{SiO}_2$) of slag based on chemical composition (Table 1) were 1.01 and 1.92, respectively.

Table 1. Physical and chemical properties of cement and slag.

Chemical Composition (wt.%)	OPC	Slag
CaO	62.89	42.66
SiO ₂	19.96	33.39
Al ₂ O ₃	4.35	15.14
Fe ₂ O ₃	3.50	0.64
MgO	2.90	6.26
Na ₂ O	0.48	0.04
K ₂ O	0.80	0.81
SO ₃	3.30	0.16
LOI	1.30	0.72
Blaine fineness (m ² /kg)	415	346
Specific gravity (kg/m ³)	2650	2980

The X-ray diffraction pattern (XRD) shown in Figure 3 indicates that slag is a predominantly amorphous material. The alkaline solution used to activate the slag was a combination of reagent grade sodium hydroxide (NaOH; SH) and water glass (liquid sodium silicate; SS). The sodium silicate used is composed of 29.3% SiO₂, 12.7% Na₂O, and 58.0% H₂O.

2.2. Specimen Preparation and Mix Proportions

A total of 20 AAS-CPB mixtures were prepared by mixing tailings, binders and water. Liquid activators were prepared 24 h before preparation of CPB specimens and allowed to cool down to room temperature (20 ± 2 °C). The required amounts of tailings, binder and water were mixed and homogenized for about 10 min by using a double spiral mixer in order to produce the desired CPB mixtures. The produced backfill mixtures were poured into beakers (500 mL). Specimens were then sealed and cured at room temperature. CPB samples made up of OPC were also prepared as control sample.

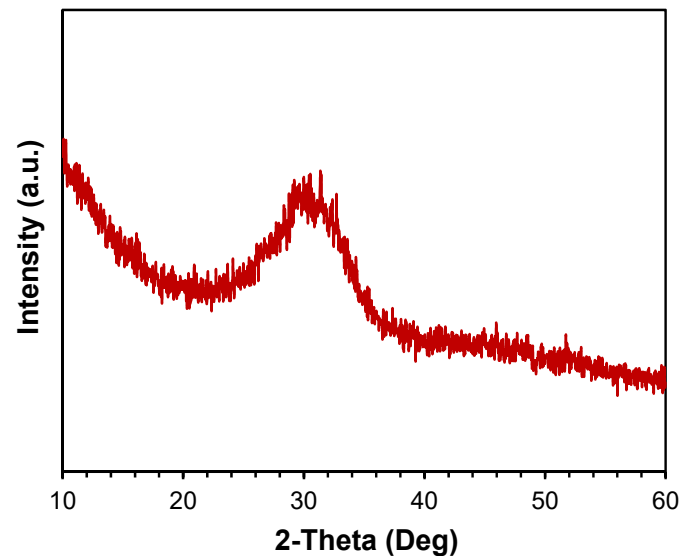


Figure 3. XRD profile of the slag sample.

After specific curing times, rheological tests were performed, as described below. The parameters investigated were the binder content, the activator dosage, M_s , and the fineness of slag. The activator dosage was kept constant for all the mixes at 16%. The detailed mix proportions are summarized in Table 2.

Table 2. Summary of the mix compositions of the specimens prepared.

CPB trial Mixtures	Used Binder Types	Binder Content (%)	Activator Dosage (%)	M_s (-)	Slag Fineness (m^2/kg)	Water Content (%)
Effect of binder content						
BC-4%	AAS	4	16	0.26	395	24.2
BC-6%	AAS	6	16	0.26	395	24.3
BC-8%	AAS	8	16	0.26	395	24.4
BC-10%	AAS	10	16	0.26	395	24.5
OPC-6%	OPC	6	-	-	-	-
Effect of silicate modulus						
M_s -0.18	AAS	6	16	0.18	395	24.2
M_s -0.26	AAS	6	16	0.26	395	24.3
M_s -0.34	AAS	6	16	0.34	395	24.4
M_s -0.41	AAS	6	16	0.41	395	24.4
Effect of the fineness of slag						
SF-346 m^2/kg	AAS	6	16	0.26	346	24.3
SF-395 m^2/kg	AAS	6	16	0.26	395	24.3
SF-457 m^2/kg	AAS	6	16	0.26	457	24.3
SF-573 m^2/kg	AAS	6	16	0.26	573	24.3
Effect of curing temperature						
T-10°C	AAS	6	16	0.26	395	24.3
T-20°C	AAS	6	16	0.26	395	24.3
T-30°C	AAS	6	16	0.26	395	24.3
T-40°C	AAS	6	16	0.26	395	24.3

BC: binder content, $(M_{slag} + M_{activator}) \times 100 / (M_{tailings} + M_{water} + M_{slag} + M_{activator})$; SF: fineness of slag; T: curing temperature (M: weight).

2.3. Rheological Testing

The rheological behavior of fresh CPB mixtures was measured using Brookfield RSR-SST rheometer with a four-bladed vane with a diameter of 20 mm and length of 40 mm. The test procedure typically consists of a constant 100 s^{-1} pre-shear for 30 s and a subsequent downramp where the applied shear strain rate was decreased from 100 to 0.001 s^{-1} in 60 s. The specimens were tested at 0, 0.5, 1 and 2 h after mixing. All the samples were mixed every 10 min with a spatula to ensure the homogeneity of the system. Prior to each measurement, the sample was agitated by hand for 1 min with a spatula to avoid settling of particles and to obtain a homogeneous mixture. The rheological parameters (yield stress and plastic viscosity) were determined by fitting the down-ramp data using the Bingham model, as shown in Equation (1). The Bingham model accurately represented all the CPB mixtures studied, as the coefficients of determination found for all the curves denoted good correlations.

In the equation below, τ is the shear stress (Pa), τ_0 is the yield stress (Pa), η is the plastic viscosity (Pa·s), and γ is the shear rate (s^{-1}).

$$\tau = \tau_0 + \eta\gamma \quad (1)$$

3. Results and Discussions

3.1. Effect of Binder Content

The variations in yield stress and plastic viscosity for CPB samples with different binder contents as a function of time is presented in Figure 4. A set of CPB specimens made up of OPC with a binder content of 6% was also prepared as a control sample. Note that Ms was kept constant at 0.26 for all the AAS-CPB mixtures. It can be observed from Figure 4 that irrespective of binder content, all AAS-CPB samples exhibit similar behavior, i.e., a gradual increase in both yield stress and plastic viscosity with increasing curing time. This can be well related to the consumption of water and formation of hydration products (primarily sodium and/or calcium aluminosilicate hydrates; C-A-S-H and/or N-A-S-H), which increases the interfrictional resistance of the particle assembly [39–41].

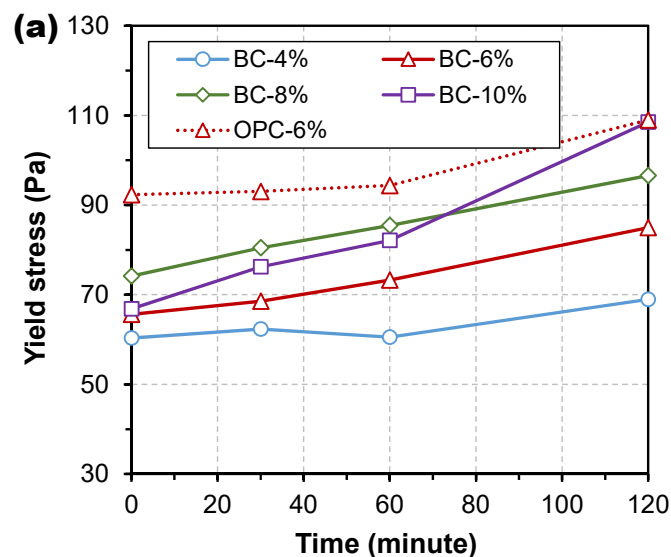


Figure 4. Cont.

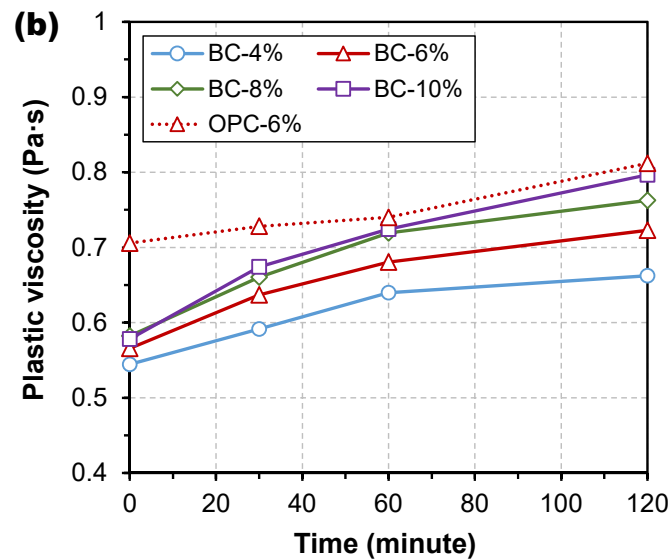


Figure 4. Yield stress (a) and plastic viscosity (b) of CPBs with different binder contents.

Figure 4 also shows that regardless of curing time, both yield stress and plastic viscosity of AAS-CPB increases with increasing binder content up to 8%. This is mainly because an increase in binder dosage results in more amount of hydration products, which, in turn, enhances the rheological behavior of CPB during shearing. However, it is interesting to notice that a further increase in binder content from 6% to 8% yields lower yield stresses and plastic viscosities during the first 1 h. The possible explanation is that higher replacement of mine tailings and with liquid activator and higher negative zeta potential slag results in lower number of direct particle-particle contacts and stronger particle dispersion and, thus leading to better flowability. These observations indicate that there is a competition between the rheology-increasing factor (higher amount of hydration products with increasing binder) and rheology (yield stress and plastic viscosity)-decreasing factor (stronger repulsive particle-particle force and larger distance between particles). The results presented in Figure 4 also show that the AAS-CPB with higher binder content experiences a higher rate of gain in both yield strength and plastic viscosity.

From Figure 4a, it can be well observed that the time-dependent rheological behavior of AAS-CPB samples is significantly different than that of CPB made up of OPC. AAS-CPB samples show consistently lower yield stress and plastic viscosity values (by 19–29%) than OPC-CPB samples. The results shown in Figure 4a also indicate that the rate of gain in rheological parameters of AAS-CPB samples appear to be much higher than that for OPC-CPB samples. For instance, the BC-6% sample experiences a 29% increase in yield stress during the 2h curing while yield stress increases by 14% for OPC-6% sample. This observation can be mainly attributed to the fact that the hydration reaction of AAS is more intense than that of OPC.

3.2. Effect of Silicate Modulus

AAS-CPB samples with various Ms ratios (0.18, 0.26, 0.34 and 0.41) were prepared at a fixed binder content of 6% and an activator dosage of 16%. An activator dosage of 16% was chosen deliberately since it gives the highest compressive strength. The influence of Ms on the yield stress and plastic viscosity of the AAS-CPB samples as a function of time is illustrated in Figure 5. From this figure, it is evident that both yield stress and plastic viscosity increase with an increase in the curing time. As explained previously, this can be well attributed to the ongoing hydration of AAS binder.

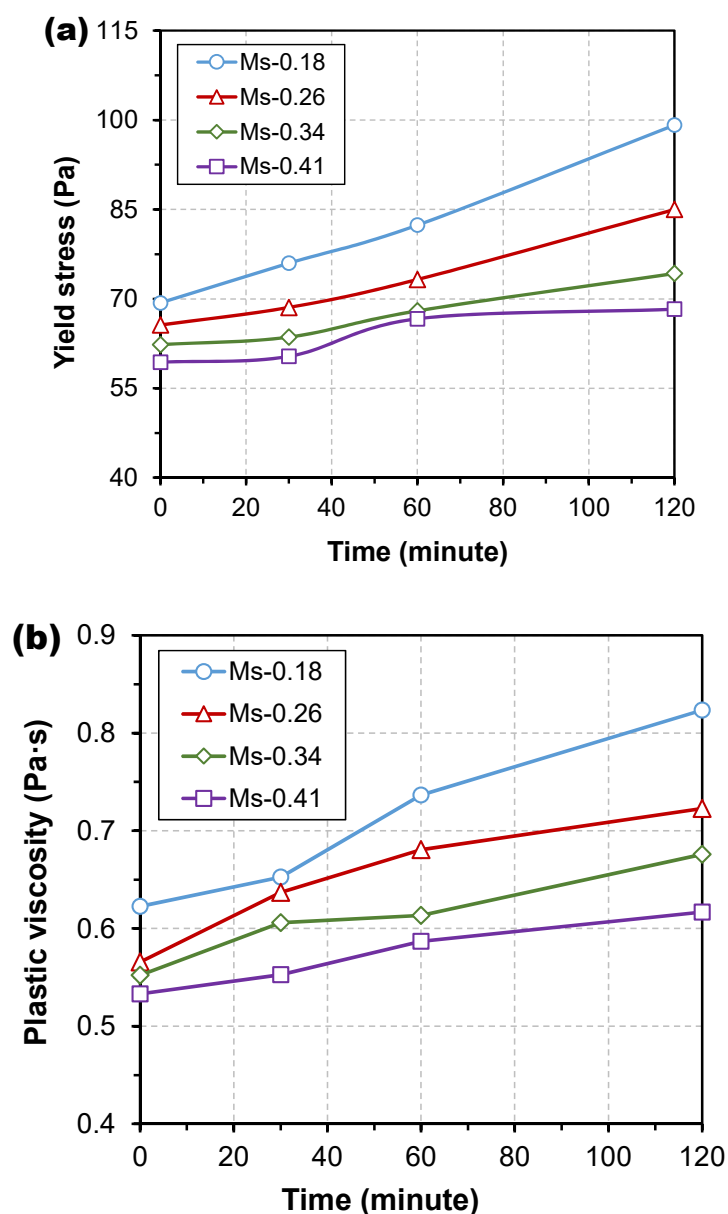


Figure 5. Effect of Ms on the yield stress (a) and plastic viscosity (b) of CPB.

Figure 5 also shows that the AAS-CPB sample with lower Ms has consistently greater yield stress and plastic viscosity, especially at later age. Moreover, the rate of gain in yield stress and plastic viscosity appears to increase with decreasing Ms. For instance, within 2 h after mixing, the yield stress of the AAS-CPB samples with Ms of 0.41, 0.34, 0.26 and 0.18 increases by 15%, 19%, 30% and 43%, respectively, while the corresponding plastic viscosity increases by 16%, 22%, 27% and 32%, respectively. These observations can be mainly explained by the fact that at the same activator dosage, alkali activator with lower Ms has greater pH value, thus resulting in higher rate of hydration reaction of the AAS binder and subsequent more amount of hydration products. An additional factor should also be considered as a contributor to the lower yield stress and plastic viscosity of AAS-CPB with higher Ms. This factor is an increase in silicate species in activator can result in more negative zeta potential, as negatively charged silicate species from the activator can absorb or precipitate on the slag particle surfaces [41]. This contributes to increasing the repulsive particle-particle force and thus decreasing the yield stress and plastic viscosity.

3.3. Effect of the Fineness of Slag

Previous studies [18,42,43] argue that increasing the fineness of slag within a certain range improves the compressive strength of the AAS-based materials. In tests, the effect of the fineness of slag on the evolution of the rheological properties was evaluated (Figure 6). AAS-CPB samples made of slags with a fineness of 346, 395, 457 and 573 m²/kg are prepared at a fixed binder content of 6% and Ms of 0.26. From Figure 6, it is obvious that the increase in the slag-specific surface from 346 to 573 m²/kg produces an increase in the yield stress and plastic viscosity and this effect is more pronounced at later age. These observations can be explained by the fact that the increase in the fineness of the slag favors the reactivity of slag, thus leading to the formation of higher amount of hydration products and the consumption of more free water.

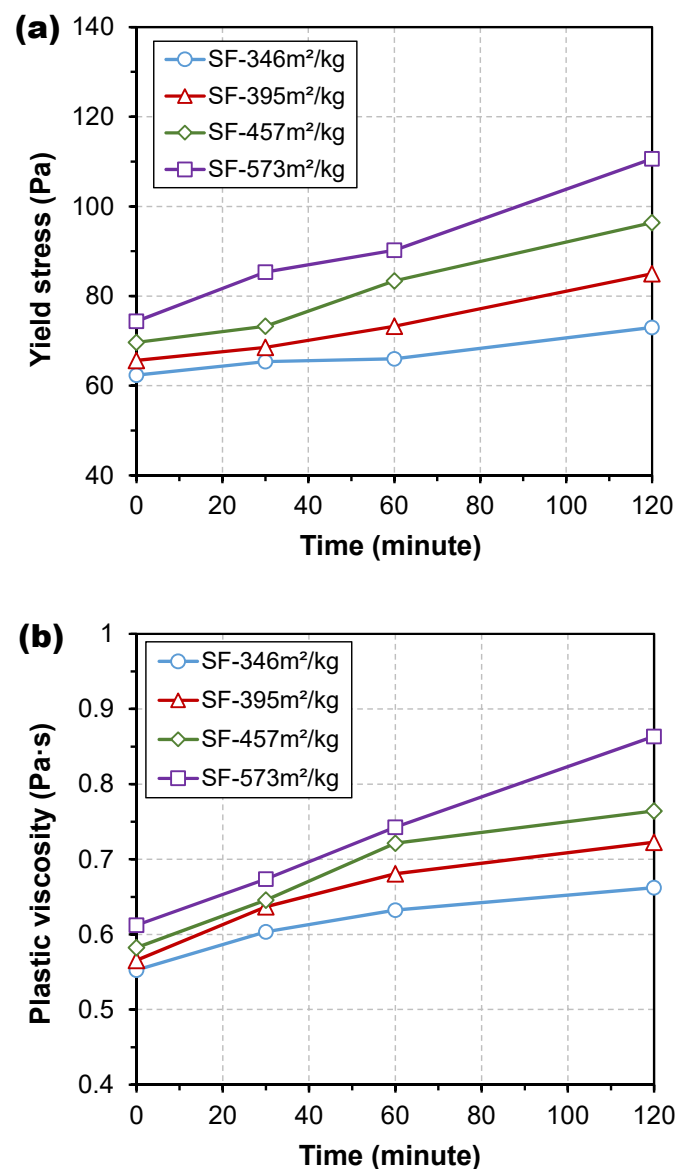


Figure 6. Effect of the fineness of slag on yield stress (a) and plastic viscosity (b) of CPB.

In addition, slag with a higher specific surface means there is more surface area to be wetted [44], which in turn reduces the effectiveness of the lubrication of free water during shearing and thus the flowability of the system. The results presented above indicate that aside from the strength, the rheological properties of AAS-CPB should also be carefully examined in the determination of the

optimum fineness of slag. Moreover, AAS-CPB sample made of higher specific surface slag shows a higher rate of gain in both yield stress and plastic viscosity. For instance, the yield stress increases by 17%, 29%, 38% and 48% for slags with fineness of 346, 395, 457 and 573 m²/kg within the same timeframe (2 h), while the corresponding increment in plastic viscosity is 20%, 27%, 31% and 41%, respectively.

3.4. Effect of Curing Temperature

Every single underground mine is unique with regards to its temperature conditions [45]. The effect of curing temperature on the development of the yield stress and plastic viscosity of CPBs over a curing period of 2 h is clearly illustrated in Figure 7. The binder content, M_s and fineness of slag were kept constant for all AAS-CPB samples at 6%, 0.26 and 395 m²/kg, respectively. OPC-CPBs with the binder content of 6% were prepared as reference. From Figure 7, it is obvious that regardless of binder type and curing age, CPBs exposed to an elevated curing temperature produce higher yield stress and plastic viscosity and faster rate of gain in these rheological parameters. The cogent reason for this is that a higher temperature accelerates the hydration of binders, thus resulting higher amount of hydration products [45–47].

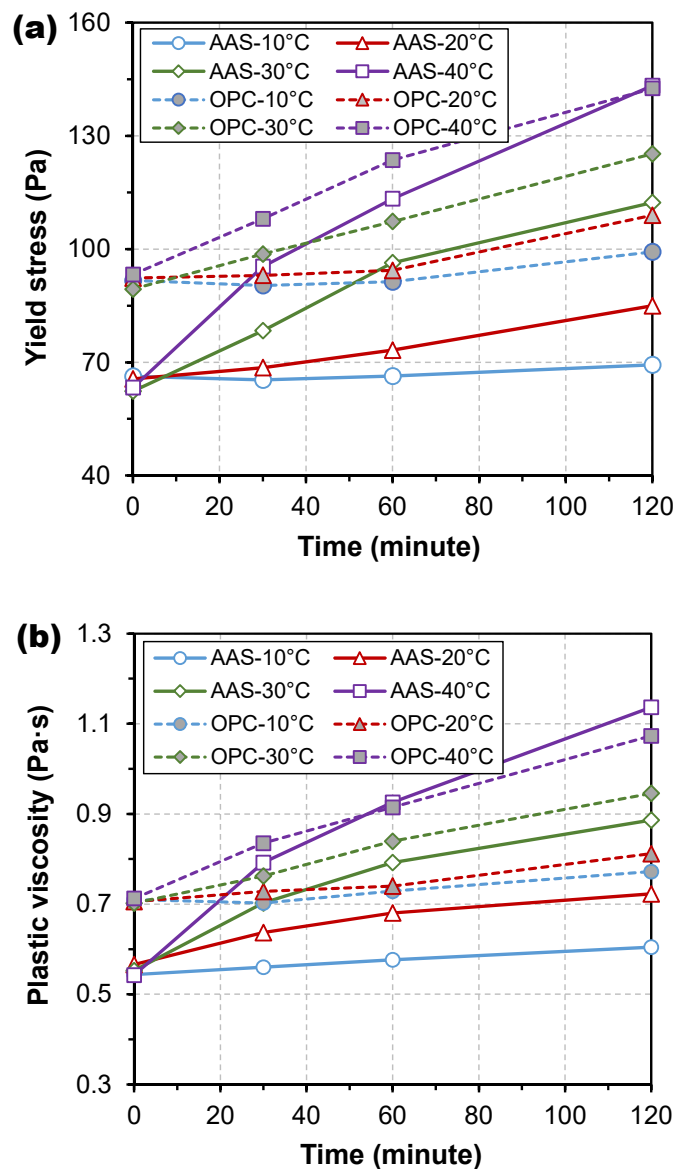


Figure 7. Time-dependent evolution of yield stress (a) and plastic viscosity (b) of CPB.

From Figure 7, it can be also noticed that the significance of the influence on AAS-CPB and OPC-CPB is quite different. To better illustrate this difference, the percent increases in both yield stress and plastic viscosity within the same timeframe (2 h) are plotted versus the corresponding curing temperature, as shown in Figure 8. It can be clearly seen that as the curing temperature increases, the percent increase in both yield stress and plastic viscosity of AAS-CPBs within 2 h increases at a higher rate than those of OPC-CPBs. This finding indicates that the yield stress and plastic viscosity of AAS-CPB is more sensitive than that of OPC-CPB to curing temperature.

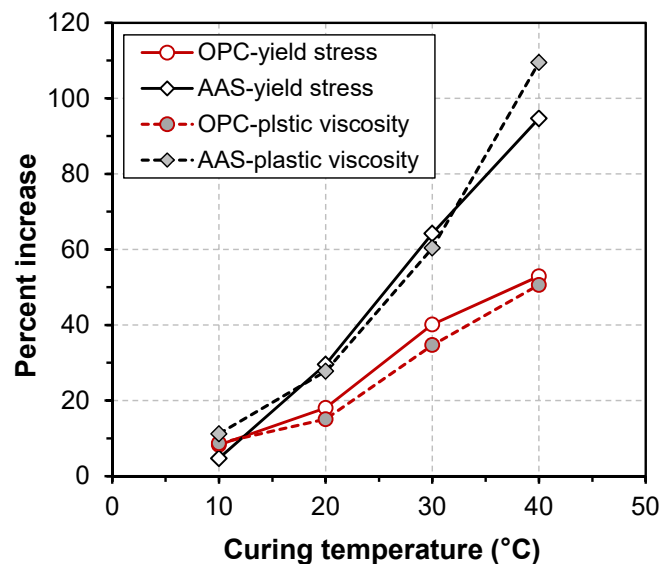


Figure 8. The rate of gain in yield stress and plastic viscosity of CPBs cured at different temperatures.

4. Conclusions

This paper investigates experimentally the effect of binder content, M_s , the fineness of slag and curing temperature on the rheological properties of AAS-CPB mixtures prepared with an activator dosage of 16 wt.%. Based on the experimental results obtained, the following conclusions are made:

- Both yield stress and plastic viscosity of AAS-CPB samples gradually increases with the curing time due to the consumption of water and formation of hydration products that introduce new inter-particle forces.
- The yield stress and plastic viscosity of AAS-CPBs increases with increasing binder content up to 8%, while a further increase in binder content results in a decrease in the initial yield stress and plastic viscosity. An increase in binder content accelerates the rate of gain in both yield stress and plastic viscosity. Both yield stress and plastic viscosity of AAS-CPB are consistently lower than those of OPC-CPB with the same binder content.
- AAS-CPB sample with lower M_s has consistently greater yield stress and plastic viscosity and the rate of gain in these parameters. This can be well attributed to the lower pH value of pore solution and higher negative zeta potential of solid particles at higher M_s .
- Increasing in the slag-specific surface from 346 to 573 m²/kg produces a consistent increase in both yield stress and plastic viscosity. The AAS-CPB sample made of higher specific surface slag shows a higher rate of gain in both yield stress and plastic viscosity.
- Both OPC- and AAS-CPBs exposed to an elevated curing temperature produce higher yield stress and plastic viscosity and faster rate of gain in these rheological parameters. AAS-CPBs are found to be more sensitive to the variation in curing temperature than OPC-CPBs with respect to the rate of gain in yield stress and plastic viscosity.

In the present study, only the laboratory-scale rheological test was considered. However, it was known that the field conditions should be reflected by CPB-surrounding rock interactions. In the future research, the placement and curing conditions (e.g., stress application) of CPB–rock interactions will be investigated thoroughly. As a result, the findings of this study can provide critical technical data and information to mine backfill operators or engineers for the handling, delivery, and placement of the AAS-CPB materials.

Author Contributions: Conceptualization, Y.K. and H.J.; Methodology, L.R.; Formal Analysis, L.R. and Y.L.; Investigation, Y.K. and H.J.; Writing—Original Draft Preparation, Y.K. and H.J.; Validation, Writing—Review & Editing, E.Y., L.R. and Y.L.; Visualization, all. All authors have read and agreed to the published version of the manuscript.

Funding: This research was financially supported by National Natural Science Foundation of China (51804063) and China Postdoctoral Science Foundation (2019M652426).

Conflicts of Interest: The authors declare no conflict of interest. The funders had no role in the design of the study; in the collection, analyses, or interpretation of data; in the writing of the manuscript, or in the decision to publish the results.

References

1. Belem, T.; Benzaazoua, M. Design and application of underground mine paste backfill technology. *Geotech. Geol. Eng.* **2008**, *26*, 147–174. [[CrossRef](#)]
2. Cao, S.; Yilmaz, E.; Song, W. Dynamic response of cement-tailings matrix composites under SHPB compression load. *Constr. Build. Mater.* **2018**, *186*, 892–903. [[CrossRef](#)]
3. Kesimal, A.; Yilmaz, E.; Ercikdi, B.; Alp, I.; Devenci, H. Effect of properties of tailings and binder on the short-and long-term strength and stability of cemented paste backfill. *Mater. Lett.* **2005**, *59*, 3703–3709. [[CrossRef](#)]
4. Yilmaz, E.; Belem, T.; Benzaazoua, M. Study of physico-chemical and mechanical characteristics of consolidated and unconsolidated cemented paste backfills. *Miner. Resour. Manag.* **2013**, *29*, 81–100. [[CrossRef](#)]
5. Yilmaz, E.; Benzaazoua, M.; Belem, T.; Bussi ere, B. Effect of curing under pressure on compressive strength development of cemented paste backfill. *Miner. Eng.* **2009**, *22*, 772–785. [[CrossRef](#)]
6. Pokharel, M.; Fall, M. Combined influence of sulphate and temperature on the saturated hydraulic conductivity of hardened cemented paste backfill. *Cem. Concr. Compos.* **2013**, *38*, 21–28. [[CrossRef](#)]
7. Jiang, H.; Han, J.; Li, Y.; Yilmaz, E.; Sun, Q.; Liu, J. Relationship between ultrasonic pulse velocity and uniaxial compressive strength for cemented paste backfill with alkali-activated slag. *Nondestruct. Test. Eval.* **2019**. In-press. [[CrossRef](#)]
8. Ouattara, D.; Mbonimpa, M.; Yahia, A.; Belem, T. Assessment of rheological parameters of high density cemented paste backfill mixtures incorporating superplasticizers. *Constr. Build. Mater.* **2018**, *190*, 294–307. [[CrossRef](#)]
9. Jiang, H.; Yi, H.; Yilmaz, E.; Liu, S.; Qiu, J. Ultrasonic evaluation of strength properties of cemented paste backfill: Effects of mineral admixture and curing temperature. *Ultrasonics* **2020**, *100*, 105983. [[CrossRef](#)]
10. Yan, B.; Zhu, W.; Hou, C.; Yilmaz, E.; Saadat, M. Characterization of early age behavior of cemented paste backfill through the magnitude and frequency spectrum of ultrasonic P-wave. *Constr. Build. Mater.* **2020**, *249*, 118733.
11. Cao, S.; Yilmaz, E.; Song, W. Fiber type effect on strength, toughness and microstructure of early age cemented tailings backfill. *Constr. Build. Mater.* **2019**, *223*, 44–54. [[CrossRef](#)]
12. Hassani, F.; Razavi, S.M.; Isagon, I. A study of physical and mechanical behaviour of gelfill. *CIM Bull.* **2007**, *100*, 1–7.
13. Pokharel, M.; Fall, M. Coupled thermochemical effects on the strength development of slag-paste backfill materials. *J. Mater. Civ. Eng.* **2010**, *23*, 511–525. [[CrossRef](#)]
14. Li, W.C.; Fall, M. Strength and self-desiccation of slag-cemented paste backfill at early ages: Link to initial sulphate concentration. *Cem. Concr. Compos.* **2018**, *89*, 160–168. [[CrossRef](#)]
15. Yilmaz, E.; Kesimal, A.; Ercikdi, B. The factors affecting the strength and stability of paste backfill. *Yerbilimleri Bull. Earth Sci.* **2003**, *28*, 155–169.

16. Xue, G.; Yilmaz, E.; Song, W.; Yilmaz, E. Influence of fiber reinforcement on mechanical behavior and microstructural properties of cemented tailings backfill. *Constr. Build. Mater. Constr.* **2019**, *213*, 275–285. [[CrossRef](#)]
17. Cihangir, F.; Akyol, Y. Mechanical, hydrological and microstructural assessment of the durability of cemented paste backfill containing alkali-activated slag. *Int. J. Min. Reclam. Environ.* **2016**, *32*, 1–21. [[CrossRef](#)]
18. Cihangir, F.; Ercikdi, B.; Kesimal, A.; Ocak, S.; Akyol, Y. Effect of sodium-silicate activated slag at different silicate modulus on the strength and microstructural properties of full and coarse sulphidic tailings paste backfill. *Constr. Build. Mater.* **2018**, *185*, 555–566. [[CrossRef](#)]
19. Nguyen, L.; Moseson, A.; Farnam, Y.; Spatari, S. Effects of composition and transportation logistics on environmental, energy and cost metrics for the production of alternative cementitious binders. *J. Clean. Prod.* **2018**, *185*, 628–645. [[CrossRef](#)]
20. Fernández-Jiménez, A.; Palomo, J.G.; Puertas, F. Alkali-activated slag mortars mechanical strength behavior. *Cem. Concr. Res.* **1999**, *29*, 1313–1321. [[CrossRef](#)]
21. Shi, C.; Krivenko, P.V.; Roy, D. *Alkali-Activated Cements and Concretes*; Taylor and Francis, CRC Press: Boca Raton, FL, USA, 2006; 392p.
22. Bakharev, T.; Sanjayan, J.G.; Cheng, Y.B. Resistance of alkali-activated slag concrete to acid attack. *Cem. Concr. Res.* **2003**, *33*, 1607–1611. [[CrossRef](#)]
23. Bakharev, T.; Sanjayan, J.G.; Cheng, Y.B. Sulfate attack on alkali-activated slag concrete. *Cem. Concr. Res.* **2002**, *32*, 211–216. [[CrossRef](#)]
24. Komljenovic, M.; Bašcarevic, Z.; Marjanovic, N.; Nikolic, V. External sulfate attack on alkali-activated slag. *Constr. Build. Mater.* **2013**, *49*, 31–39. [[CrossRef](#)]
25. Qiu, J.; Zhao, Y.; Long, H.; Guo, Z.; Xing, J.; Sun, X. Low-carbon binder for cemented paste backfill: Flowability, strength and leaching characteristics. *Minerals* **2019**, *9*, 707. [[CrossRef](#)]
26. Xue, G.; Yilmaz, E.; Song, W.; Cao, S. Compressive strength characteristics of cemented tailings backfill with alkali-activated slag. *Appl. Sci.* **2018**, *8*, 1537. [[CrossRef](#)]
27. Jiang, H.Q.; Qi, Z.J.; Yilmaz, E.; Han, J.; Qiu, J.P.; Dong, C.L. Effectiveness of alkali-activated slag as alternative binder on workability and early age compressive strength of cemented paste backfills. *Constr. Build. Mater.* **2019**, *218*, 689–700. [[CrossRef](#)]
28. Haruna, S.; Fall, M. Time- and temperature-dependent rheological properties of cemented paste backfill that contains superplasticizer. *Powder Technol.* **2020**, *360*, 731–740. [[CrossRef](#)]
29. Qiu, J.; Guo, Z.; Yang, L.; Jiang, H.; Zhao, Y. Effects of packing density and water film thickness on the fluidity behaviour of cemented paste backfill. *Powder Technol.* **2020**, *359*, 27–35. [[CrossRef](#)]
30. Xiao, B.; Wen, Z.; Wu, F.; Li, L.; Yang, Z.; Gao, Q. A simple L-shape pipe flow test for practical rheological properties of backfill slurry: A case study. *Powder Technol.* **2019**, *356*, 1008–1015. [[CrossRef](#)]
31. Bharathan, B.; McGuinness, M.; Kuhar, S.; Kermani, M.; Hassani, F.P.; Sasmito, A. Pressure loss and friction factor in non-Newtonian mine paste backfill: Modelling, loop test and mine field data. *Powder Technol.* **2019**, *344*, 443–453. [[CrossRef](#)]
32. Yang, L.; Yilmaz, E.; Li, J.W.; Liu, H.; Jiang, H.Q. Effect of superplasticizer type and dosage on fluidity and strength behavior of cemented tailings backfill with different solid contents. *Constr. Build. Mater.* **2018**, *187*, 290–298. [[CrossRef](#)]
33. Cao, S.; Yilmaz, E.; Song, W.D. Evaluation of viscosity, strength and microstructural properties of cemented tailings backfill. *Minerals* **2018**, *8*, 352. [[CrossRef](#)]
34. Mangane, M.B.C.; Argane, R.; Trauchessec, R.; Lecomte, A.; Benzaazoua, M. Influence of superplasticizers on mechanical properties and workability of cemented paste backfill. *Miner. Eng.* **2018**, *116*, 3–14. [[CrossRef](#)]
35. Cheng, H.; Wu, S.; Li, H.; Zhang, X. Influence of time and temperature on rheology and flow performance of cemented paste backfill. *Constr. Build. Mater.* **2020**, *231*, 117117. [[CrossRef](#)]
36. Wu, D.; Fall, M.; Cai, S.J. Coupling temperature, cement hydration and rheological behaviour of fresh cemented paste backfill. *Miner. Eng.* **2013**, *42*, 76–87. [[CrossRef](#)]
37. Sultana, A.; Valouma, A.; Bartzas, G.; Komnitsas, K. Properties of inorganic polymers produced from brick waste and metallurgical slag. *Minerals* **2019**, *9*, 551. [[CrossRef](#)]
38. Komnitsas, K.; Yurramendi, L.; Bartzas, G.; Karmali, V.; Petrakis, E. Factors affecting co-valorization of fayalitic and ferronickel slags for the production of alkali activated materials. *Sci. Total Environ.* **2020**, *721*, 137753. [[CrossRef](#)]

39. Li, Z.; Ohkubo, T.A.; Tanigawa, Y. Theoretical analysis of time-dependence and thixotropy of fluidity for high fluidity concrete. *J. Mater. Civ. Eng.* **2004**, *16*, 247–256. [[CrossRef](#)]
40. Li, Z.; Ohkubo, T.A.; Tanigawa, Y. Yield model of high fluidity concrete in fresh state. *J. Mater. Civ. Eng.* **2004**, *16*, 195–201. [[CrossRef](#)]
41. Kashani, A.; Provis, J.L.; Qiao, G.G.; Deventer, J.S.J. The interrelationship between surface chemistry and rheology in alkali activated slag paste. *Constr. Build. Mater.* **2014**, *65*, 583–591. [[CrossRef](#)]
42. Wang, S.D.; Scrivener, K.L.; Pratt, P.L. Factors affecting the strength of alkali-activated slag. *Cem. Concr. Res.* **1994**, *24*, 1033–1043. [[CrossRef](#)]
43. Shi, C.J.; Li, Y.Y. Investigation on factors affecting the characteristics of alkali-phosphorous slag cement. *Cem. Concr. Res.* **1989**, *19*, 527–533.
44. Fall, M.; Benzaazoua, M.; Ouellet, S. Experimental *characterization* of the influence of tailings fineness and density on the quality of cemented paste backfill. *Miner. Eng.* **2005**, *18*, 41–44. [[CrossRef](#)]
45. Cao, S.; Yilmaz, E.; Xue, G.; Yilmaz, E.; Song, W. Loading rate effect on uniaxial compressive strength behavior and acoustic emission properties of cemented tailings backfill. *Constr. Build. Mater.* **2019**, *213*, 313–324. [[CrossRef](#)]
46. Jiang, H.Q.; Fall, M. Yield stress and strength of saline cemented tailings in sub-zero environments: Portland cement paste backfill. *Int. J. Miner. Process.* **2017**, *160*, 68–75. [[CrossRef](#)]
47. Jiang, H.Q.; Fall, M.; Cui, L. Yield stress of cemented paste backfill in sub-zero environments: Experimental results. *Miner. Eng.* **2016**, *92*, 141–150.



© 2020 by the authors. Licensee MDPI, Basel, Switzerland. This article is an open access article distributed under the terms and conditions of the Creative Commons Attribution (CC BY) license (<http://creativecommons.org/licenses/by/4.0/>).